Effect of magnetic ordering on the optical properties of transition-metal halides: $NiCl_2$, $NiBr_2$, $CrCl_3$, and $CrBr_3$

L. Nosenzo and G. Samoggia
Dipartimento di Fisica "A. Volta," Università degli Studi di Pavia
e Gruppo Nazionale di Struttura della Materia del Consiglio Nazionale delle Ricerche, I-27100 Pavia, Italy

I. Pollini
Dipartimento di Fisica, Università degli Studi di Milano, I-20133 Milano, Italy
e Gruppo Nazionale di Struttura della Materia del Consiglio Nazionale delle Ricerche, I-20133 Milano, Italy
(Received 6 July 1983)

New reflectance and thermoreflectance spectra, in the (3–9)-eV region of ferromagnetic $CrBr_3$ and antiferromagnetic $CrCl_3$, $NiCl_2$, and $NiBr_2$, insulators are reported. Changes in the optical spectra near the magnetic transition temperature have been observed. In particular, below T_c, the main optical structures of $CrBr_3$ are split into two components $\simeq 0.1$ eV apart. This finding is shown to agree with the Kerr-effect data reported in the literature. While the first charge-transfer transitions (A_1) begins to split above T_c, the splitting of the higher-energy bands follows the macroscopic magnetization law. This different behavior is attributed to a different localization of the electronic states. Antiferromagnetic crystals do not show any band splitting. Their complex phenomenology is discussed in some detail.

I. INTRODUCTION

During the last few years, the optical properties of magnetic semiconductors and insulators in the high-absorption region (beyond the *d-d* or *f-f* crystal-field transitions) have been intensively investigated. Many ferromagnetic (FM) and antiferromagnetic (AFM) crystals belonging to different families, such as europium chalcogenides,[1] spinels MCr_2X_4 (M=Cd, Hg; X=S, Se), chromium chalcogenides,[2] transition-metal halides,[3] and magnetic oxides,[4] have been carefully studied. In particular, attention has been focused upon the optical effects induced near the transition temperature (T_c or T_N) by the onset of magnetic order. Early absorption measurements[5,6] revealed the most characteristic effect of the FM transition, i.e., the "anomalous" red shift of the transmission edge. This effect has been associated with the splitting of the optical edge, a feature which is also displayed by a number of electronic transitions beyond the edge.[7]

The thermoreflectance (TR) technique has proved particularly suited to study the temperature behavior of spectra in magnetic crystals, because it displays the spectral changes induced by temperature variations. Abrupt changes of TR line shapes and a strong increase in signal intensity are generally observed near T_c or T_N.[2,8–15] These facts, added to the experimental simplicity of the TR technique and the possibility of using polarized light,[16] justify its intensive use for optical studies of magnetic crystals.

While thermal lattice expansion and electron-phonon interaction are fully responsible for the TR signals in nonmagnetic semiconductors or insulators,[17] in magnetic crystals the occurrence of critical behaviors near T_c or T_N puts in evidence the leading role of magnetic phenomena. The exchange interaction and the critical fluctuations of the spin ordering have been shown to be, in some FM and AFM crystals,[10,11,18] the microscopic mechanisms of thermal modulation, resulting in "splitting" and "broadening" TR line shapes. In other cases, optical changes may be due to oscillator strength transfer and, in AFM crystals, to the reduced symmetry of the magnetic lattice.[18] A number of phenomena has been explained only qualitatively, namely the existence of unsplit optical bands showing red-shift coefficients,[3,10,11] band splittings in AFM crystals,[10,19,20] or optical effects due to short-range exchange interaction.[10–14] Some of these phenomena seem to support the concept that optical transitions, through the electron-spin interaction, probe a magnetic environment the size of which depends upon the specific excitation involved.[8]

In order to use TR studies to identify the optical transitions, it is necessary to have a correct interpretation of the TR signal and some theoretical knowledge of energy levels and electron-spin interactions. In such a case, quantitative analyses of the TR spectra have been shown to be viable.[8,21] On the other hand, in most cases analyses of the TR spectra have been very approximate. As regards the energies of the electronic levels, great difficulties arise from the coexistence of localized and itinerant-electron states.[22–26] This is why in magnetic insulators there is a lack of safe theoretical provisions. Also for the second problem, i.e., that of the interaction between the excited electron and the ion spin system, a satisfactory solution is not in sight. Many theoretical works have dealt with this problem by envisioning an itinerant electron interacting with the magnetic ions (*s-d* or *s-f* model).[22–26] In other cases, the model of an electron localized around the excited magnetic ion has been shown to account satisfactorily

for some experimentals results.[27] However, a comprehensive theoretical model for interpreting the optical behavior of the different magnetic crystals is still lacking.

In this situation, we think that a systematic experimental study of extended optical spectra of magnetic compound families should be very useful. To this aim, we now report a rather complete experimental study of reflectivity (R) and TR spectra of four transition-metal halides (ferromagnetic $CrBr_3$ and antiferromagnetic $CrCl_3$, $NiBr_2$, and $NiCl_2$) near the magnetic phase transition. This work complements a previous study of the paramagnetic (PM) optical properties of these crystals.[3]

In Sec. II the principles for application of the TR techniques to magnetic crystals will be summarized, in order to aid the interpretation of the results which will be analyzed in Sec. IV. Section III will be dedicated to the description of nontrivial experimental details. Finally, the discussion of the results is presented in Sec. V.

II. THERMOREFLECTANCE LINE SHAPES

It is well known[28] that an optical structure in the reflectivity spectrum can generally be described by a local dielectric function $\epsilon=\epsilon(\epsilon_\infty, \nu_0, \Gamma, f, \text{and } \nu)$, where ν_0, Γ, and f indicate the resonance frequency, the broadening parameter, and the oscillator strength, respectively, of the associated electronic transition. Their temperature dependence determines the behavior of the optical structure and also its TR line shape.

In the case of nonmagnetic semiconductors or insulators, it has been shown that the expression,

$$\frac{\Delta R}{R}=\frac{1}{R}\left[\frac{dR}{d\nu_0}\frac{d\nu_0}{dT}+\frac{dR}{d\Gamma}\frac{d\Gamma}{dT}\right]\Delta T\simeq\frac{1}{R}\frac{dR}{d\nu_0}\frac{d\nu_0}{dT}\Delta T\ , \tag{1}$$

is generally appropriate to interpret the TR spectra.[29] With a very few exceptions, the fundamental optical transitions blue-shift ($d\nu_0/dT<0$) and sharpen ($d\Gamma/dT>0$) on lowering the temperature, due to the electron-phonon interaction and the lattice contraction.[17] The experimental values of $|d\nu_0/dT|$ (ranging between 10^{-3} and 4×10^{-4} eV/K) and of $d\Gamma/dT$ ($\approx10^{-4}$ eV/K) (Ref. 30) justify the approximation shown in Eq. (1) and make the TR spectra "locally" similar to the wavelength derivation of the reflectivity. As a matter of fact, a good correlation between the zero-crossing points (from positive to negative) in the TR spectrum and the energy position of the R peaks is generally found in nonmagnetic materials.

In Fig. 1(a) we report the behavior of the "shift" ($R^{-1}dR/d\nu_0$) and the "broadening" ($R^{-1}dR/d\Gamma$) spectral functions, as calculated by means of the complex dielectric constant

$$\tilde{\epsilon}=\epsilon_\infty+\frac{f}{\nu_0^2-\nu^2+i\Gamma\nu}\ . \tag{2}$$

The Lorentzian line reproduces well the shape of the optical bands due to transitions between localized states, typical of low-dielectric-constant crystals considered in this paper ($\epsilon_\infty=3$–4). We remark that the TR line shape appears shiftlike even if the broadening coefficient is of the same order or greater than the shift term. However, in this case the zero-crossing point moves to energies lower than that of the R peak. This situation is typical of the principal optical structures of $CrBr_3$ in the PM phase and the phenomenon is illustrated in Fig. 1(a), where we have plotted the

$$\frac{1}{R}\left[\frac{dR}{d\nu_0}\frac{d\nu_0}{dT}+\frac{dR}{d\Gamma}\frac{d\Gamma}{dT}\right]\left[\frac{d\nu_0}{dT}\right]^{-1}=\frac{1}{R}\left[\frac{dR}{d\nu_0}+C\frac{dR}{d\Gamma}\right]$$

function for different values of the ratio $C=|(d\Gamma/dT)/(d\nu_0/dT)|$.

In magnetic crystals, the occurrence of critical behaviors in the TR spectra near or below the phase transition temperature gives evidence of predominant magnet-

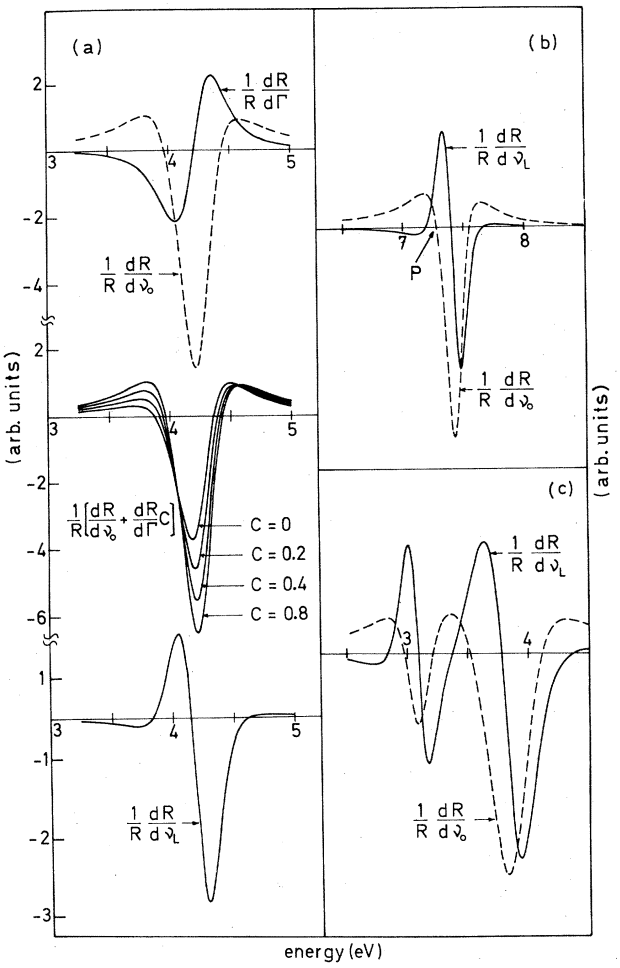

FIG. 1. Thermoreflectance line shape associated with a damped Lorentz oscillator. In (a) we report at the top the shift and broadening TR line shapes, in the middle the evolution of a shift TR signal by increasing the broadening contribution $C=|(d\Gamma/dT)/(d\nu_0/dT)|$, at the bottom the splitting line shape. In (b) and (c) the paramagnetic (pure shift) and ferromagnetic (pure splitting) line shapes, simulating the E_1 and A_1-A_2 $CrBr_3$ structures, respectively, are reported. The following parameters have been assumed. A_1: $h\nu_0=3.03$, $hf=4.5$, $h\Gamma=0.35$, $h\nu_L=0.04$. A_2: $h\nu_0=3.55$, $hf=12$, $h\Gamma=0.55$, $h\nu_L=0.04$, $\epsilon_\infty=6$. E_1: $h\nu_0=7.34$, $hf=4$, $h\Gamma=0.26$, $h\nu_L=0.04$, $\epsilon_\infty=3$.

ic contributions to the TR signals. In many cases it has been shown that an accurate analysis of the signal line shape allows one to determine the predominant modulation mechanisms.[10,11,21]

Shift or broadening of optical structures, associated to a critical behavior, have been observed in many AFM crystals[10,11] by TR techniques. Since the spectral functions $R^{-1}dR/d\nu_0$ and $R^{-1}dR/d\Gamma$ in Eq. (1) are nearly temperature independent, the critical behavior of the signal intensity must be ascribed to the temperature dependence of the coefficients $d\nu_0/dT$ and $d\Gamma/dT$. The magnetic contributions can be written explicitly through

$$\frac{d\nu_0}{dT}=\frac{d\nu_0}{dM}\frac{dM}{dT} \quad \text{and} \quad \frac{d\Gamma}{dT}=\frac{d\Gamma}{dM}\frac{dM}{dT} .$$

Here, as in the following, M indicates either the macroscopic or the sublattice magnetization or any other local-order parameter, depending on the specific electronic transition considered.

In FM crystals, due to the strong exchange interaction, a splitting of the optical structures below T_c has been observed in many cases.[7,8,12–15] Generally, a structure can split in many components which are different with respect to polarization and shift coefficients. Thus, a general treatment of the splitting TR line shape is complex. However, in a previous paper[21] we have shown that, by using a simple model, it is possible to account for the main features of the FM splitted 7.3-eV optical band in $CrBr_3$. In that case, we assumed that a classical Lorentz model describes well the electronic transition of interest. A magnetic field representing the effects of the spin ordering splits the optical band in two symmetrical and circularly polarized (cp) components. The temperature modulation ΔT of the magnetization M (the molecular field) produces a correspondent variation $\Delta\nu_L$ of the splitting energy ν_L. The TR spectrum, calculated by means of the dielectric constant,[21]

$$\epsilon_{\pm}=\epsilon_{\infty}+\frac{f}{\nu_0^2-\nu^2\pm 2\nu\nu_L+i\Gamma\nu} , \tag{3}$$

and the relations

$$R=\tfrac{1}{2}(R_{+}+R_{-}) ,$$
$$\frac{\Delta R_{\pm}}{R_{\pm}}=\frac{1}{R_{\pm}}\left[\frac{dR_{\pm}}{d\nu_L}\frac{d\nu_L}{dM}\frac{dM}{dT}\right]\Delta T , \tag{4}$$

are shown in Fig. 1(a).

We remark that for $\nu_L \ll \Gamma$, the unpolarized TR signal takes the shape of the second derivative of R with respect to the energy. This line shape appears whenever an optical band begins to split, independently of the number and the polarization of its components, as can be seen by analyzing the TR spectra of a number of crystals reported in literature.[8,15]

As a last comment, we observe that in many cases, when T crosses T_c, a TR shift modulation coefficient is overcome by the splitting term. If we suppose that a blue-shift mechanism is operative in the PM phase ($CrBr_3$ case), then, in a suitable interval near T_c, the TR signal consists of two contributions,

$$\Delta R=(\Delta R)_{\text{shift}}+(\Delta R)_{\text{splitting}} . \tag{5}$$

As the FM splitting mechanism begins to operate, the TR line shape starts to change and, in particular, the point P [see Fig. 1(b)] shifts towards high energies and stops when the intensity of the splitting term overcomes the shift contribution. In this way, a plot of point-P energy versus T gives a qualitative indication for the onset of the splitting mechanism in the examined optical structure. As long as $\nu_L < \Gamma$, lowering the temperature does not change the line shape and the signal intensity is governed by the function $\nu_L(T)$ [or $M(T)$]. More precisely, since the function $dR/d\nu_L$ ($\nu_L \ll \Gamma$) is linear with ν_L, then

$$\Delta R\simeq\frac{dR}{d\nu_L}\Delta\nu_L\simeq\nu_L\Delta\nu_L=\tfrac{1}{2}\Delta[(\nu_L)^2] . \tag{6}$$

So we can extract the ν_L value (i.e., the exchange integral J) and the dependence of $\nu_L(T)$ from the λ-shape intensity curves. More direct information on ν_L could be obtained by measuring the polarized TR spectrum with the sample in a saturating magnetic field.[16]

III. EXPERIMENTAL

Since a general description of the vacuum ultraviolet apparatus and the experimental layout was given previously,[3] we discuss only some aspects of the measurement techniques which are relevant in this work.

Thermomodulation was obtained by means of indirect heating. The samples (4×4 mm^2, 0.1—0.3 mm thick) were put into contact with the heater by means of a film of silicon grease. Heating was accomplished with a thin germanium plate resistor ($4\times10\times0.2$ mm^3, $\sim1\ \Omega$) and a low-frequency (1.5-Hz) square-wave current generator.

Temperatures were measured by means of a gold—2.11 at. %-Co versus silver—0.37 at. %-Au thermocouple, kept on the front surface of the heater and electrically insulated from it. The amplitude of the sample thermal modulation ΔT was obtained by measuring the rms value of the first harmonic of the synchronous variation induced in the emf of the thermocouple. On taking TR spectra, temperature modulation between 0.1 and 1 K has been used, depending on temperature range and light level employed. When studying the behavior versus T of the intensity of the TR signal, modulations between 0.05 and 0.1 K were sufficient.

The sample cooling was obtained by means of a Cryotip refrigerator manufactured by Air Products, working in back pressure ($T<33$ K, $T>80$ K) or in flux equilibrium conditions (33 K $<T<$ 80 K). Temperature fluctuations, in the time required to signal-average a whole TR spectrum, were ±0.5 and ±1.5 K in back-pressure and flux equilibrium conditions, respectively. When measuring the signal intensity versus T, the data were taken point by point by varying the back pressure, or continuously, during the cryostat warming up. Good agreement between the two procedures was found. Absolute determination of the sample temperature is somewhat uncertain due to thermal gradients and to the fact that temperature is not read on the spot where the beam is collimated. Gradients

are mainly induced by the thermomodulation power and are estimated to be smaller than ± 1.5 K in the spectra measurements and ± 0.5 K, when measuring the signal intensity. However, we estimate that the finite dimension of the light spot on the crystal surface (1×2 mm^2), assured a good thermal homogeneity of the surface studied, better than 0.2 K.

The reflectivity was measured by means of a double beam, double photomultiplier optical system. The signal processing system employed two lock-in amplifiers, an analogic ratiometer, and a final integrator to enhance the sensitivity. The correction of the zero line was made *a posteriori*. The frequency derivative of the reflectivity, $dR/d\nu$, was derived from the R data.

IV. ANALYSIS OF THE EXPERIMENTAL RESULTS

The analysis of the experimental results presented in this section is based on the comparison between the R (or $dR/d\nu$) and the TR spectra and, further, on the concepts introduced in Sec. II. All the R and TR spectra presented have been obtained with unpolarized light. We remark that the sign of the TR curves has been determined according to that of $R^{-1}(dR/dT)$. In Fig. 2 we report the R spectra of all the crystals studied for the reader's convenience. In Table I we also report the energy positions of the main bands and the modulation mechanisms which characterize the TR structures. In the following we present a detailed discussion of the features of R and TR spectra.

A. $CrBr_3$

The most salient characteristic of the behavior of the TR spectrum of $CrBr_3$ is the net line-shape change which occurs in the main optical bands A_1, A_2, and E_1, going from the PM to the FM phase. This effect is illustrated in Fig. 3, where the experimental TR spectrum of the A_1, A_2, and E_1 structures is shown in both phases.

It was formerly suggested[21] that a symmetric splitting mechanism could reproduce well the unpolarized TR line shape in the case of the E_1 band. Later, by means of TR measurements using cp light in Faraday disposition,[16] it has been experimentally proved that the above assumption applies to description of the A_1 transition. For this reason, we show in Figs. 1(b) and 1(c) the spectra in the A_1-A_2 and E_1 regions, as calculated with the model presented in Sec. II, and the assumption that in the PM and FM phases blue shift and splitting mechanism are operative, respectively. Since the behavior of the A_2 and E_1 structures appears similar to that of A_1 as regards both the line shape and intensity, we suggest that in the FM phase the symmetric splitting in two bands is the dominant thermal effect for all the mentioned bands of $CrBr_3$. For the A_1 and E_1 structures, this effect can also be observed in the R spectrum (see Fig. 4). However, notice that the TR spectra, through the line-shape change, display the effect more strongly and allow one to follow it when $T \to T_c$.

To further characterize the transitions, we report in Fig. 5(a) the behavior of the zero-crossing point P for the A_1 and A_2 structures. In the $T/T_c \gtrsim 2$–3 region the plots indicate a blue shift of the optical structures, while at lower temperatures the saturation indicates the establishment of a splitting line shape. Notice that the A_1 and A_2 bands have also a different behavior versus T, with the A_2 band behaving as the E_1 band.

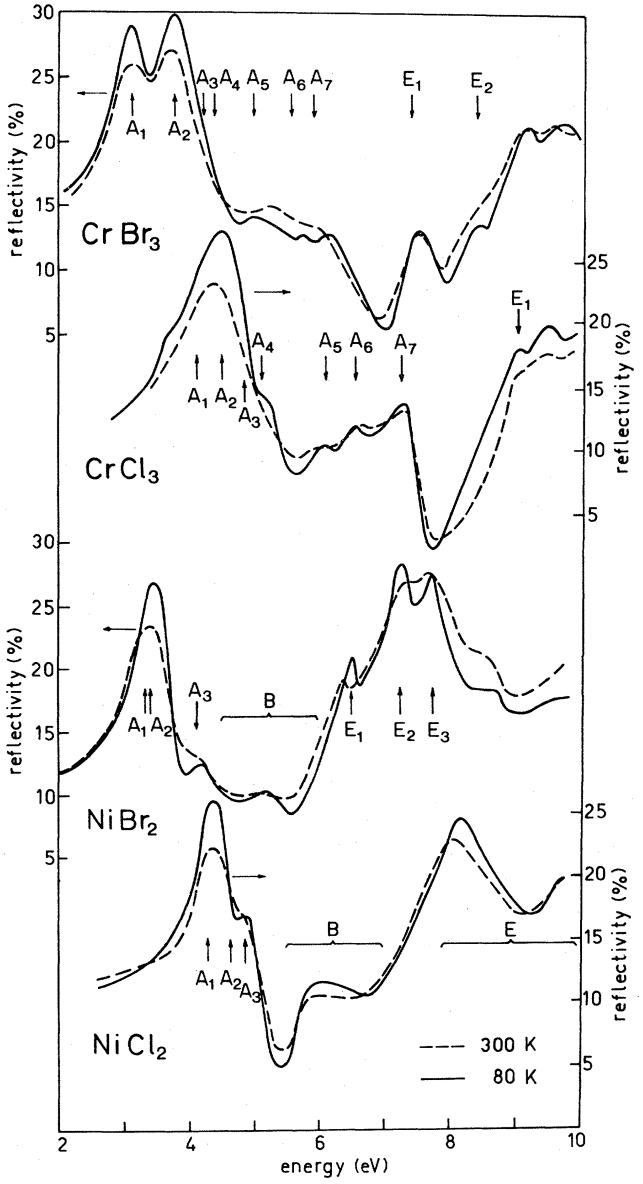

FIG. 2. Reflectivity spectra of chromium and nickel bromides and chlorides at 80 K (full line) and 300 K (dashed line), taken from Ref. 3. Peaks and structures have been again labeled with capital letters A, B, and E.

In Fig. 5(b) we report the peak-to-peak intensity of the TR signal for the A_1 and E_1 structures as a function of T. These λ-shaped curves put in evidence the critical behavior of the spectra reproduced in arbitrary scale in Fig. 6. By using these λ curves and Eq. (6), the behavior of the splitting energy ν_L vs T can be followed in Fig. 5(c).

TABLE I. Transition energies and predominant TR line shapes of the main optical structures in the paramagnetic and ferromagnetic (antiferromagnetic) phases. Most of the transition energies have been determined from the R peaks at 80 K. The energies marked with an asterisk (*) are derived from the TR spectra at 80 K, while those with two asterisks (**) are relative to TR measurements at 30 K.

	$CrBr_3$		$CrCl_3$			$NiBr_2$			$NiCl_2$	
	$T > T_c$	$T < T_c$	$h\nu$ (eV)	$T > T_N$	$T < T_N$	$h\nu$ (eV)	$T > T_N$	$T < T_N$	$h\nu$ (eV)	$T > T_N$	$T < T_N$
A_1	3.05	blue shift	splitting	A_1	4.15*	blue shift	blue shift	A_1	3.45*	broadening	broadening	A_1	4.37	broadening	red shift
A_2	3.75	blue shift	splitting	A_2	4.45	blue shift	broadening	A_2	3.65*	broadening	red shift	A_2	4.75**	broadening	broadening
A_3	4.00**			A_3	4.75*		broadening	A_3	4.20			A_3	4.85		
A_4	4.15*			A_4	5.15			B_1	4.65*			B_1	5.70*		
A_5	4.90			A_5	6.10			B_2	5.05*			B_2	6.10		
A_6	5.65			A_6	6.52			B_3	5.20			B_3	6.75*		
A_7	6.05			A_7	7.25			B_4	6.00*			B_4	7.40*		
E_1	7.35	blue shift	splitting	E_1	9.05			E_1	6.50	blue shift	broadening	E_1	8.17	blue shift	broadening
E_2	8.20			E_2	9.50			E_2	7.25	broadening	red shift	E_2	10		
E_3	9.05							E_3	7.74	broadening	broadening				
								E_4	8.5						

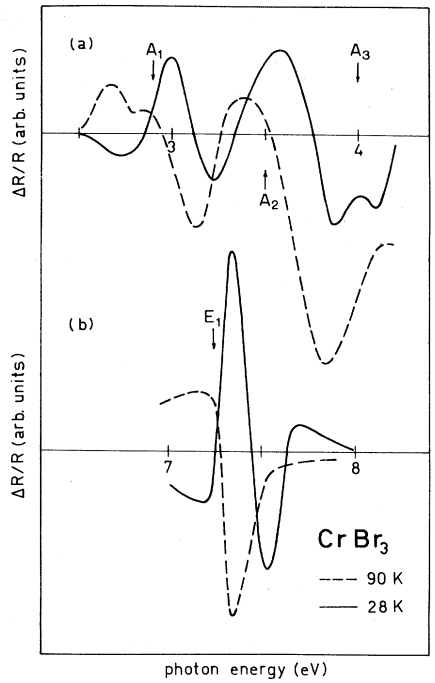

FIG. 3. Thermoreflectance spectra of $CrBr_3$ in the para- and ferromagnetic phases. The arrows drawn in the figure denote the 90-K zero-crossing points for the bands A_1, A_2, A_3, and E_1.

B. $CrCl_3$

The broad band centered at nearly 4.5 eV is very sensitive to temperature changes. Its linewidth (~ 1 eV) as well as the modifications which appear on lowering T (see Fig. 7) indicate the complex character of this structure.

In order to establish the number of the component bands, we have examined the frequency derivative $dR/d\nu$ spectrum (Fig. 8). It appears that in this region three optical bands coexist, A_1, A_2, and A_3. The fact that the whole $dR/d\nu$ spectrum evolves without sudden changes to the AFM phase reflects a continuous evolution of the R spec-

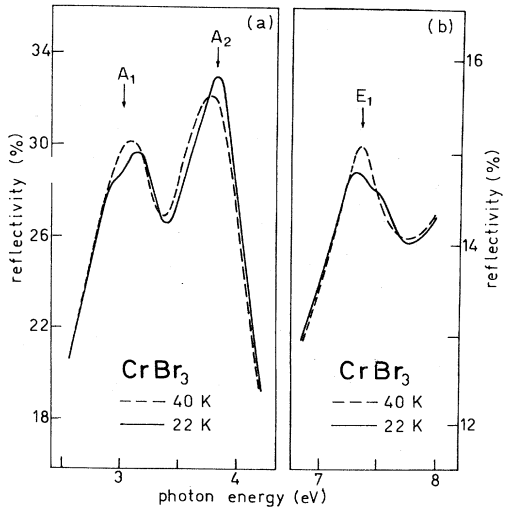

FIG. 4. Reflectivity spectra of $CrBr_3$ in the region of the bands A_1, A_2, and E_1 above and below T_c (32.5 K). The splittings of the bands A_1 and E_1 are observable.

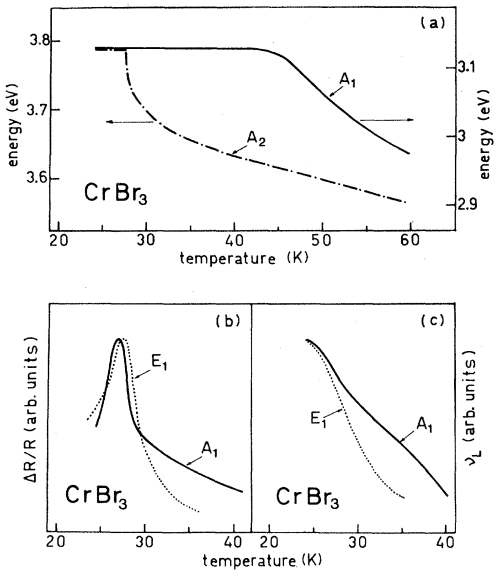

FIG. 5. Critical behavior of (a) the zero-line crossing points, (b) of the TR modulation intensity $\Delta R/R$, and (c) the splitting frequency ν_L, for the structures A_1, A_2, and E_1 of $CrBr_3$ around the Curie point.

trum on lowering T: The A_1 component blue-shifts, A_2 appears still, and A_3 gets stronger.

Inspection of the TR spectrum (Fig. 8) yields further information about these bands. For example, in the PM phase the whole TR signal is dominated by the A_1 and A_2 structures, which between 90 and 20 K blue-shift and sharpen. In the AFM phase, the contribution of the A_2

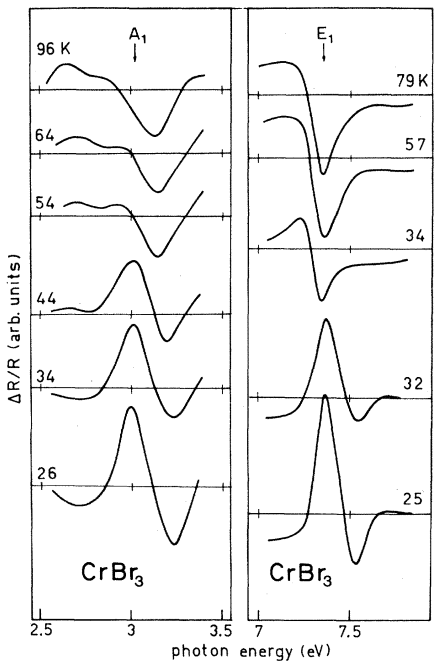

FIG. 6. Thermoreflectance spectra of the A_1 and E_1 bands of $CrBr_3$ at different temperatures in paramagnetic and ferromagnetic phases. Notice that the line shape changes for the A_1 and E_1 structures occur around 45 and 33 K, respectively.

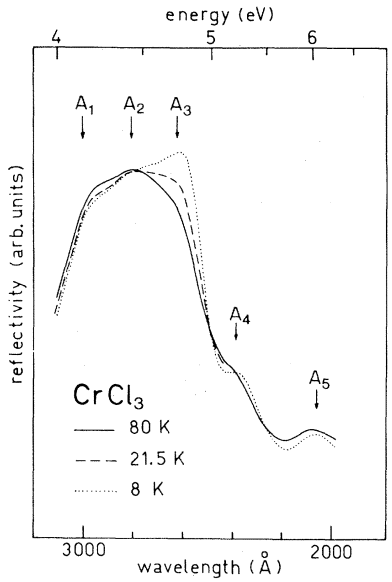

FIG. 7. Reflectivity spectrum of $CrCl_3$ in the region of the bands A_1 to A_5 above and below T_N (16.8 K).

structure becomes suddenly negligible in comparison to that of A_1 and A_3, which show blue shift and broadening ($d\Gamma/dT > 0$), respectively. Note that, while the line-shape change takes place in less than one degree near T_N, the intensity of the signal increases with continuity by a factor

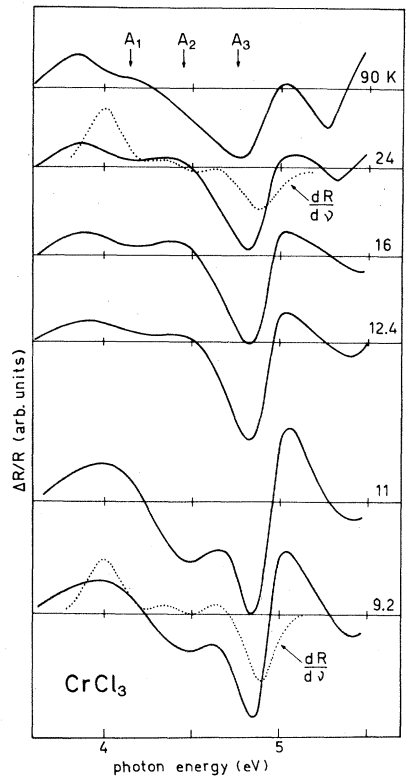

FIG. 8. Thermoreflectance spectra of the A_1, A_2, and A_3 bands of $CrCl_3$ at fixed temperatures in the paramagnetic and antiferromagnetic phases. The spectra of the function $dR/d\nu$ (dotted line) above (24 K) and below (9.2 K) T_N are also reported.

of 3 from 25 to 12 K, in accordance with a λ curve centered near T_N.

C. $NiBr_2$

The main structures of $NiBr_2$ are grouped in two different regions of the spectrum. The first one, the "charge-transfer" region, is situated between 3 and 4 eV. It consists of a complex structure which is shown in detail in Fig. 9(a). Two main components located at about 3.45 (A_1) and 3.55 (A_2) eV can be separated in the $dR/d\nu$ spectrum of Fig. 10. Besides detecting this phenomenon, the TR spectra present the following features: In the PM phase the zero-crossing points of $dR/d\nu$ correspond to the negative minima of the TR spectrum: The whole line shape is typical of a broadening mechanism ($d\Gamma/dT>0$) operative in both the A_1 and A_2 bands. In the AFM phase, the A_2 band takes a red-shift line shape. This change is gradual and saturates at about 40 K.

The second region between 6 and 8 eV contains three main optical bands, E_1, E_2, and E_3.

E_1. By analyzing the R spectra at various temperatures, the E_1 band appears to blue-shift up to about 50 K. On the contrary, in the AFM phase it sharpens while maintaining its position [Fig. 9(b)]. This behavior is reflected in the line-shape change of the TR spectrum between 50 and 60 K (Fig. 10).

E_2–E_3: Concerning these structures, good agreement exists in the PM phase between the R peak (zero crossing of the $dR/d\nu$ curve) and the negative TR minima, signaling broadening TR line shape. Below 50 K, the E_2 band red-shifts in the R spectra. The corresponding TR signal changes gradually to a red-shifted line shape which saturates at 40 K. The E_3 band position does not change on lowering T. The enhancement of the R peak is rather due to band sharpening: In effect this band keeps in the AFM phase the TR broadening line shape.

In conclusion, we remark that all the bands examined show near T_N a slight increase in the TR signal intensity, 2–3 times the PM value, regardless of the change of the modulation mechanism.

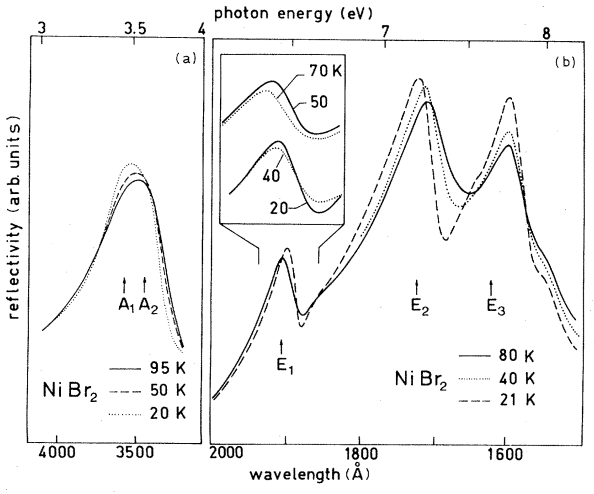

FIG. 9. Reflectivity spectrum of $NiBr_2$ in the charge-transfer region (A_1 and A_2 bands) and the excitonic region (E_1 to E_3 bands) above and below T_N (60 K).

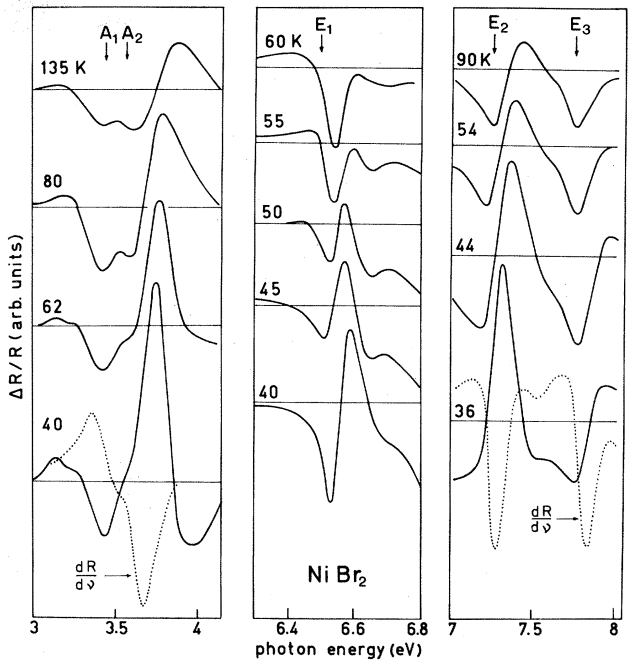

FIG. 10. Thermoreflectance spectra of the A_1, A_2, and E_1, E_2, and E_3 bands of $NiBr_2$ at different temperatures in the para- and antiferromagnetic phases. The functions $dR/d\nu$ (dotted line) are also reported.

D. $NiCl_2$

The charge-transfer region of $NiCl_2$ presents a complicated pattern of superimposed bands (Fig. 2). The TR spectra are not reproduced because they do not differ substantially from those shown in Fig. 3 of Ref. 3. The main results are listed in Table I.

V. DISCUSSION

In a previous paper[3] the reported R spectra of Cr and Ni halides were discussed in terms of charge-transfer and excitonic transitions. Two energy regions can be identified: region I (from 3 to 6 eV), where A and B bands are assigned to $3d^n \rightarrow p^5$ (halogen) $3d^{n+1}$ (metal) charge-transfer transitions, and region II (from 6 to 10 eV), where the sharp E peaks are attributed to excitonic transitions. Concerning nickel halides, further support to the assignment of the A bands to charge-transfer processes can be obtained from the comparative study of the optical properties of transition-metal ions. In fact, in compounds where these ions are present either as bivalent impurities in large-band-gap crystalline matrices ($KMgF_3$, MgF_2, LiCl) or as components of divalent crystals,[31–35] the energy difference between regions I and II decreases in going from the electronic configuration d^8 (Ni^{2+}) to d^5 (Mn^{2+}). This behavior agrees with band-structure calculations for some layered transition-metal halides.[36–38] Few experimental data exist for chromium compounds and we have no knowledge of any correlations established with other

trivalent ion salts. However, likewise NiX_2 crystals, CrX_3 ($X=$Cl, Br) show the presence of two separated regions in the R spectra. This suggests to attribute the first group of A bands in chromium halides to charge-transfer transitions.

We will now comment on the changes of the optical spectra occurring in the magnetic phase. The difficulty of finding a suitable theoretical framework to account for these phenomena makes our discussion mostly phenomenological. Because the spectra of FM and AFM crystals behave differently, the two groups of materials will be analyzed separately.

A. Ferromagnetic crystals

In the case of $CrBr_3$ the main optical structures (A_1, A_2, E) split symmetrically below T_c into two components showing red and blue shift, respectively. The splitting value is in the (0.1—0.2)-eV range for all bands. Splittings of the same order of magnitude have been reported for other crystals, namely, the ferromagnetic semiconductors, $HgCd_2S_4$, $CdCr_2Se_4$,[2] EuO, and EuS.[1] Such large values cannot be attributed to exchange splitting of the ground state, which in $CrBr_3$ results to be only a few meV.[39] Instead, we believe that these effects arise from exchange splitting of the energy levels of photoexcited electrons, much more spread over neighbor ions and thus more sensitive to the magnetic ordering.[40]

Some years ago, Dillon *et al.*[39] introduced a molecular-orbital model for the unpaired spins of the chromium ions, in order to interpret the dichroic splitting of the charge-transfer edge of $CrBr_3$. It was assumed that the energy-level splittings responsible for the magnetic rotation arise from the spin-orbit interaction of the final state, with negligible contribution from the applied magnetic field and the exchange field. With this assumption, the energy splittings should be temperature independent. Besides, the spin-orbit splitting, as estimated for the $CrBr_3$ charge-transfer edge, is of the order of 0.01 eV. Thus Dillon's model is inconsistent with the temperature evolution and the order of magnitude of the energy splittings we have observed. Furthermore, Yung[41] presented Kerr rotation data in the (2—3.5)-eV range, which he tried to interpret on the basis of the Dillon's model. In order to account for an unexpectedly large effect, he was compelled to hypothesize the existence of a ghost band (π band), characterized by a high magnetic activity, which was not detected by reflectivity because of its weak oscillator strength. Actually, if we assume that the exchange field causes a 0.1-eV splitting of the A_1 and A_2 bands, we can reproduce fairly well the Kerr rotation data (see Fig. 11.) Details of such calculations are given in the Appendix.

An interesting observation is that different bands show different temperature evolutions. In particular, note [Figs. 5(b) and 5(c)] that the splitting of the A_1 band begins at 45 K ($\simeq\frac{3}{2}T_c$) while A_2 and E bands start splitting at $\simeq$33 K ($\sim T_c$). In addition, the A_1 splitting at T_c is 30% of the 24 K splitting,[42] while A_2 and E splittings closely follow the temperature dependence of the macroscopic magnetization M. The different behavior of A_1 band, with respect to A_2 and E bands, is likely to rest on a different localization of the excited states: more localized for the A_1, delocalized for the other two bands. The excited electron in a localized state will experience some local order also above T_c. In fact, this electron will contribute by itself to increase the interaction between nearest ions, leading to formation of a microregion where the spins are aligned above T_c. On the contrary, itinerant electrons essentially experience the long-range order and line up only for $T<T_c$.

A point of view different from the local description[39] is presented by the so-called s-f (or s-d) model[23,24] which considers the f or d electrons (spin S_i) as localized and the conduction-band electrons (spin $\sigma=\pm\frac{1}{2}$) as itinerant. The interaction between these two systems is of the type: $H_{sf}=-g\sum_i \vec{\sigma}_i\cdot\vec{S}_i$. When the s-f interaction is small, the conduction band is split twice (spin up and spin down). The splitting energy is proportional to the macroscopic magnetization, plus a second-order shift proportional to the short-range order. This model succeeded in explaining the red shift of the absorption edge. However, some authors[21,22,26] conclude that the perturbative approach should be reconsidered and cast some doubts on the pure spin-polarized bands. In effect they showed that, in some limiting cases, the s-f model can be solved exactly, giving evidence of the existence at all temperatures (also for $T>T_c$) of a multiband structure for the conduction band built on mixed spin states. The multiband sequence should be observed if the coupling constant g of the Hamiltonian operator H_{sf} is of the same order of the bandwidth W. The energy position, the broadening, and the transition intensity should then be functions of the temperature.[21,22] Nolting interpreted the spectrum of anomalous transmission in EuS (Ref. 43) and the photoemission experiment of spin polarized electrons[44] in terms of the multiband model.[22] However, in the case of $CrBr_3$ we have not observed any effect pointing to the existence of a multiband structure. Since for the observed optical structures it is $g\ll W$ [i.e., $g<0.1$ eV, $W>1$ eV (Ref. 36)] it is almost impossible to detect single multiband ef-

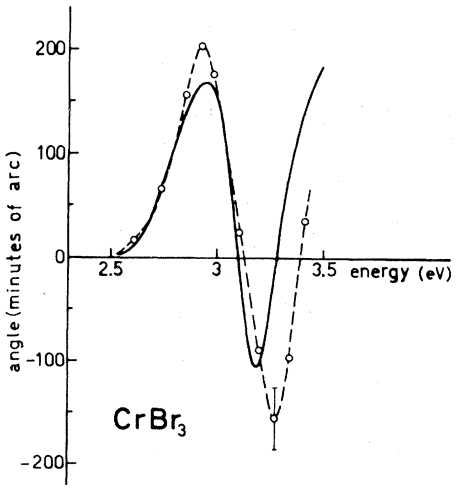

FIG. 11. $CrBr_3$ experimental Kerr rotation data taken from Ref. 41 (dotted line) compared with the spectrum calculated by supposing a ferromagnetic band splitting of 0.12 eV (solid line).

fects. In this scheme, our results could only reveal the shift of the center of gravity of the spin-up with respect to the spin-down bands.

B. Antiferromagnetic crystals

The temperature evolution of R and TR spectra of antiferromagnetic $CrCl_3$, $NiCl_2$, and $NiBr_2$ is more complicated than that observed in ferromagnetic $CrBr_3$. For this reason, we will limit the discussion to the main features of TR spectra above and below T_N.

We remark, at first, that almost all of the TR structures change their dominant modulation mechanism near T_N (see Table I); the modulation intensity also changes, showing a fairly sharp peak near T_N. These facts point to an unusual behavior of the energy and width of the optical transitions correlated to the magnetic phase transition. For example, let us consider the E_1 structure peaked at 6.2 eV in $NiBr_2$ spectrum (Fig. 10). In the paramagnetic region an analysis of TR intensity and line shape shows that blue shift is the dominant mechanism and that $d\nu_0/dT$ increases sharply as $T \rightarrow T_N$, while $d\Gamma/dT$ gives a negligible contribution. Below T_N, the broadening alone accounts for TR intensity and line shape, $d\Gamma/dT$ being positive and increasing as $T \rightarrow T_N$. The temperature behavior of E_1 band parameters ν_0 and Γ is illustrated in Fig. 12. Similar considerations can be easily extended to the other optical structures of the AFM crystals.

It has been suggested[18] that the doubling of periodicity due to antiferromagnetism introduces extra energy gaps at the new boundaries of the reduced magnetic Brillouin zone (BZ). Experimental evidence of a splitting of some bands has been reported for some optical transitions in EuTe both by TR (Ref. 11) and Faraday measurements.[19] However, in our spectra no evidence of band splitting in the AFM phase has been found. This fact suggests that only transitions not affected by the refolding of the BZ induced by the periodicity change (mostly those occurring near the center of the zone) could be responsible for the observed optical structures.

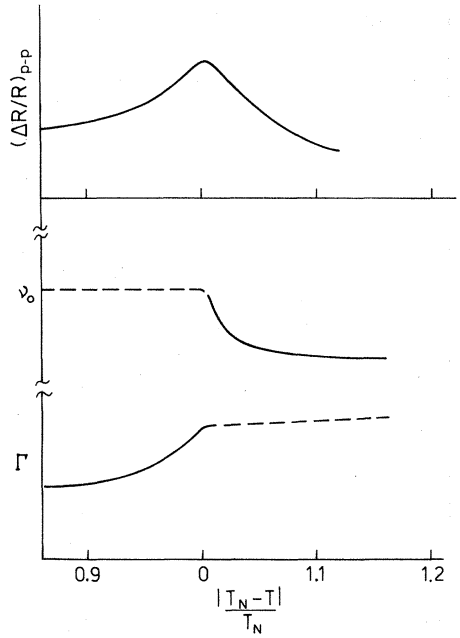

FIG. 12. At the top, the intensity of the E_1 TR signal in $NiBr_2$ is reported vs the reduced temperature $(T_N - T)/T_N$. At the bottom, a qualitative sketch of the temperature evolution of the ν_0 and Γ parameters, deduced from the evolution of TR line shape (Fig. 10), is reported for the same band.

We stress that we did not find evidence of structures with negative $d\Gamma/dT$ above T_N. On the other hand, negative broadening coefficients have been observed by Mitani and Koda[10,11] for some TR structures in Eu chalcogenides. They interpreted the increase of the critical damping Γ, when the temperature goes down to T_N, as a dynamical spin-fluctuation effect.

As a final remark we call attention to the existence, in the two nickel halides, of pairs of bands undergoing the same critical change. In the excitonic region of both crystals, the E_1 band blue-shifts at high T but broadens below T_N, while in the charge-transfer region the two main bands A_1 and A_2 have the same behavior in the two nickel halides, but with a reversed order. This fact requires that the wave functions of the ground and final states for the above mentioned pairs of optical transitions are nearly the same in both nickel crystals and justifies the notation used in this paper for labeling the optical bands. Concerning the hypothesis that two different regions should be identified in the nickel spectra, we observe that corresponding band pairs always belong to the same optical region. In addition, we note that optical bands belonging to the same region, such as the three excitonic E bands or the two charge-transfer bands, present different critical behaviors in the same crystal. This fact supports the idea that the effect of the magnetic interaction on the optical structures is extremely sensitive to the localization of the relevant electronic excitations and to their location in the BZ. Thus, one can conclude that an optical transition could be considered as a microscopic probe of magnetism. Its great complexity comes from the dependence on the electronic levels involved, which are coupled in different ways to the magnetic interaction and from the fact that "the probe" is not necessarily a small perturbation of the magnetic field.

ACKNOWLEDGMENTS

Thanks are due to Professor Marco Villa for a critical reading of the manuscript.

APPENDIX

The magneto-optical effects in magnetized media (Faraday effects in transmission and Kerr effect in reflection) can be derived from the dielectric permittivity tensor:[45]

$$\tilde{\epsilon} = \begin{bmatrix} \tilde{\epsilon}_1 & -i\tilde{\epsilon}_2 & 0 \\ i\tilde{\epsilon}_2 & \tilde{\epsilon}_1 & 0 \\ 0 & 0 & \tilde{\epsilon}_0 \end{bmatrix} .$$

For a normal incidence geometry, the major axis of the reflected beam is rotated by (Kerr rotation):[41]

$$\theta = \mathrm{Re}\frac{i(\tilde{N}_+ - \tilde{N}_-)}{\tilde{N}_+\tilde{N}_- - 1}, \tag{A1}$$

where $\tilde{N}_\pm \equiv n_\pm + ik_\pm = (\tilde{\epsilon}_\pm)^{1/2} = (\tilde{\epsilon}_1 \pm \tilde{\epsilon}_2)^{1/2}$ are the complex indices of refraction for the left and right circularly polarized (cp) light. They can be obtained from the knowledge of the optical constants in the paramagnetic phase and from the knowledge of the effects of the ferromagnetic ordering. In the case of a single Lorentzian band, symmetrically split by the magnetic effect in two right and left cp components, the dielectric permittivity is given by Eq. (3). In such a case θ vs ν is a symmetric dispersion curve centered at ν_0. In the (2—3)-eV region of $CrBr_3$ the overlapping of sharp bands strongly modifies such a shape. This effect can be seen in Fig. 11, where the experimental Kerr rotation data in $CrBr_3$ (Ref. 41) are compared with the θ function computed according to Eq. (A1). We assumed two overlapping Lorentzian bands reproducing the R data in the A_1-A_2 region, both split by 0.06 eV in the FM phase in agreement with R and TR data. The following parameters have been used: $h\nu_1 = 3.00$, $h\nu_2 = 3.55$, $h\gamma_1 = 0.3$, $h\gamma_2 = 0.5$ eV, $f_1 = 5$, $f_2 = 8$, $\epsilon_\infty = 5$. Despite the simplicity of the model, note that the Kerr data have been fairly well reproduced. The lack of agreement in the high-energy side of the spectrum is due to the existence of higher-energy bands which cannot be fully characterized on the basis of the experimental data available today.[4] These data derive from room-temperature ellipsometric measurements and from low-T (77 K) reflectivity measurements, which were taken in a rather narrow spectral range to provide good values of n and k.

As a last comment, note that, by putting $\Delta\tilde{N} = \tilde{N}_+ - \tilde{N}_-$, we rewrite Eq. (A1) as $\theta = f'\Delta n + f''\Delta k$ (where $\Delta n = n_+ - n_-$ and $\Delta k = k_+ - k_-$), which strongly resembles the well known expression of modulation spectroscopy[28]

$$\frac{\Delta R}{R} = g'\Delta(\mathrm{Re}\tilde{\epsilon}) + g''\Delta(\mathrm{Im}\tilde{\epsilon}) .$$

This explains why the Kerr rotation spectrum is similar to a derivative one. Furthermore, for an isolated band, the θ vs ν curve looks like that of TR broadening shown in Fig. 1(a), in spite of the fact that no direct correlation between thermoreflectivity and Kerr rotation exists.

[1] P. Wachter, in *Handbook on the Physik and Chemistry of Rare Earth,* edited by K. A. Gschneider and L. Eyring, (North Holland, Amsterdam, 1979), Vol. 1, Chap. 19.

[2] M. Iliev, J. Phys. (Paris) Colloq. 41, C5-23 (1980).

[3] G. Guizzetti, L. Nosenzo, I. Pollini, E. Reguzzoni, G. Samoggia, and G. Spinolo, Phys. Rev. B 14, 4622 (1976).

[4] J. W. Allen, in *Magnetic Oxides,* edited by D. J. Craik (Wiley, New York, 1975), p. 349.

[5] G. Busch, P. Junod, and P. Wachter, Phys. Lett. 12, 11 (1964).

[6] G. Harbeke and H. Pinch, Phys. Rev. Lett. 17, 1090 (1966); G. Harbeke, S. B. Berger, and F. P. Emmenegger, Solid State Commun. 6, 553 (1968).

[7] J. Feinleib, W. J. Scouler, J. O. Dimmock, J. Hanus, T. B. Reed, and C. R. Pidgeon, Phys. Rev. Lett. 22, 1385 (1969).

[8] T. Mitani and T. Koda, Phys. Rev. B 12, 2311 (1975).

[9] S. G. Stoyanov, M. N. Iliev, and S. P. Stoyanova, Phys. Status Solidi A 30, 133 (1975).

[10] T. Mitani and T. Koda, Physica 86-88B, 127 (1977).

[11] T. Mitani and T. Koda, Physica 89B, 67 (1977).

[12] M. Iliev and H. Pink, Phys. Status Solidi B 93. 799 (1979).

[13] M. Iliev and T. Arai, Solid State Commun. 31, 79 (1979).

[14] S. G. Stoyanov and I. S. Gorban, Phys. Status Solidi A 56, 655 (1979).

[15] L. Nosenzo, E. Reguzzoni, G. Samoggia, G. Guizzetti, and I. Pollini, Solid State Commun. 29, 793 (1979).

[16] A. Borghesi, L. Nosenzo, I. Pollini, E. Reguzzoni, and G. Samoggia, in *Proceedings of the VI International Conference on Vacuum Ultraviolet Radiation Physics, Charlottesville 1980,* Extended Abstracts No. I-85; A. Borghesi, G. Guizzetti, E. Samoggia, and E. Reguzzoni, Phys. Rev. Lett. 47, 538 (1981).

[17] H. Y. Fan, Phys. Rev. 82, 900 (1951).

[18] J. C. Slater, Phys. Rev. 82, 538 (1951).

[19] J. Schoenes, Z. Phys. B 20, 345 (1975).

[20] J. Schoenes and P. Wachter, Physica 86-88B, 125 (1977).

[21] L. Nosenzo, I. Pollini, E. Reguzzoni, and G. Samoggia; Solid State Commun. 37, 541 (1981).

[22] W. Nolting, Phys. Status Solidi B 96, 11 (1979).

[23] F. Rys, J. S. Helman, and W. Baltensperger, Phys. Kond. Mater. 6, 105 (1967).

[24] C. Haas, Phys. Rev. 168, 531 (1968).

[25] E. L. Nagaev, Usp. Fiz. Nauk 117, 437 (1975).

[26] V. Szocs, V. Capek, and B. Velicky, Phys. Status Solidi B 103, 139 (1981).

[27] H. H. Chou and H. Y. Fan, Phys. Rev. B 10, 901, (1974).

[28] M. Cardona, *Modulation Spectroscopy in Solid State Physics,* edited by F. Seitz and D. Turnbull (Academic, New York, 1970), Suppl. Vol. 11.

[29] See the Proceedings of the First International Conference Spectroscopy, edited by B. O. Seraphin [Surf. Sci. 37, (1973)].

[30] Bruno Batz, in *Semiconductors and Semimetals,* edited by R. K. Willardson and A. C. Beer (Academic, New York, 1974), Vol. 9.

[31] D. Bruce Chase and D. S. McClure, J. Chem. Phys. 64, 74 (1976).

[32] J. Simonetti and D. S. McClure, Phys. Rev. B 16, 3887 (1977).

[33] R. A. Statwell and D. S. McClure, J. Chem. Phys. 70, 2081 (1979).

[34] J. Simonetti and D. S. McClure, J. Chem. Phys. 71, 793 (1979).

[35] Y. Sakisaka, T. Ishii, and T. Sagawa, J. Phys. Soc. Jpn. 36, 1365 (1974).

[36] S. Antoci and L. Mihich, Phys. Rev. B 18, 5768 (1978).

[37] S. Antoci and L. Mihich, Solid State Commun. 31, 861 (1979).

[38] S. Antoci and L. Mihich, Phys. Rev. B 21, 3383 (1980).

[39] J. F. Dillon, H. Kamimura, and J. P. Remeika, J. Chem. Phys. Solids 27, 1531 (1966).

[40] E. L. Nagaev, Phys. Status Solidi B 88, 231 (1978).

[41] W. Yung, J. Appl. Phys. 36, 2422 (1968).

[42] MTR measurements (Ref. 16) give a value of 0.11 eV for $2\nu_L$ at 24 K, then one obtains from Eq. (6) that $\nu_L \approx 0.02$ eV at T_c.

[43] J. Schoenes and W. Nolting, J. Appl. Phys. 49, 1466 (1978).

[44] E. Kisker, G. Baum, A. H. Mahan, W. Raith, and B. Reihl, Phys. Rev. B 18, 2256 (1978).

[45] M. Born, Optik (Springer, Berlin, 1933).